IEEE Access
Multidisciplinary | Rapid Review | Open Access Journal

Received February 5, 2021, accepted March 3, 2021, date of publication March 15, 2021, date of current version March 23, 2021.

Digital Object Identifier 10.1109/ACCESS.2021.3065964

Joint Minimization of Spectrum and Power in Impairment-Aware Elastic Optical Networks

KUSALA MUNASINGHE[1], M. NISHAN DHARMAWEERA[1], (Member, IEEE), UDITHA WIJEWARDHANA[1], (Member, IEEE), CHAMITHA DE ALWIS[1], (Member, IEEE), AND RAJENDRAN PARTHIBAN[2], (Senior Member, IEEE)

[1]Department of Electrical and Electronic Engineering, University of Sri Jayewardenepura, Nugegoda 10250, Sri Lanka
[2]School of Engineering, Monash University, Bandar Sunway 47500, Malaysia

Corresponding author: M. Nishan Dharmaweera (nishanmd@sjp.ac.lk)

This work was supported by the National Research Council (NRC) of Sri Lanka under Grant 18-028.

ABSTRACT Flexible-grid elastic optical networks (EONs) are widely considered as the future of next generation optical transport networks. Depleting spectral resources and increasing power consumption are two critical bottlenecks of EONs. In this paper, we propose a novel impairment-aware resource allocation scheme that jointly minimizes bandwidth waste and power consumption of EONs. The proposed scheme is presented in the form of an analytical optimization for small-sized networks. A low-complexity heuristic is then proposed for large networks. Numerical results show that by appropriately assigning the route, modulation format, and carrier frequency to each connection request, the proposed scheme significantly increases spectral efficiency and reduces power consumption in networks that handle varying traffic volumes.

INDEX TERMS Elastic optical networks, physical layer impairments, power consumption, spectrum utilization, resource allocation.

I. INTRODUCTION

BANDWIDTH requirements and power consumption of the internet continue to grow at an exponential rate due to rising popularity of bandwidth-intensive mobile applications, ultra high definition video streaming, cloud computing services, and an ever-increasing user base [1]–[6]. To accommodate this growing demand, legacy wavelength division multiplexed optical networks are gradually being upgraded into EONs, which are shown to reduce cost, power consumption, and bandwidth waste, while increasing network throughput [1], [7]–[10]. The enabling technologies of EONs, such as bandwidth-variable wavelength cross-connects and transceivers as well as novel resource allocation schemes and standards, are thus being developed by researchers, vendors, and international standardization bodies [2], [4], [11]–[13].

Spectral efficiency and power consumption are often considered as important performance metrics of an EON. By increasing spectral efficiency, an EON can be designed to handle more traffic using fewer fiber resources [7], and thus, reduce capital expenditure (CAPEX). To increase spectral efficiency of an EON, a traffic connection is only assigned a set of consecutive spectrum slots (i.e., sub-carriers) that are appropriately modulated to facilitate ''just enough'' bandwidth [3]–[5], [14]. However, as these spectrum slots are spaced at a finer granularity, linear and non-linear physical layer impairments (PLIs) arise among co-propagating traffic connections [4], [5], [15]. Thus, in recent years, researchers have developed novel routing, modulation and spectrum allocation (RMSA) schemes to increase the spectral efficiency of EONs while countering the effect of impairments. The impairment-aware RMSA schemes presented in [7], [8], [16], and [17] estimate PLIs using the Gaussian Noise GN) model and allocate resources accordingly. These PLI-aware RMSA schemes increase spectral efficiency while reducing the bandwidth blocking ratio and, thereby, allow core networks to accommodate a large traffic volume with limited resources [4], [11].

Power consumption has a profound effect on the operational cost (OPEX) of an optical transport network [2], [12], [18], [19]. Especially in large core networks, where resources are provisioned to serve peak-hour traffic,

The associate editor coordinating the review of this manuscript and approving it for publication was Rene Essiambre.

a significant amount of power is consumed even during off-peak hours [2], [18], [20]–[22]. Power consumption of such networks can be reduced by dynamically adjusting the capacity of the network resources [12], [18], [20]–[23].

Although spectral efficiency [7], [8], [24]–[28] and power consumption [18], [29]–[33] have been separately optimized in many studies, to the best of our knowledge, none of those schemes can jointly optimize these quantities while accounting accurately for impairments. Therefore, in this paper, we propose a novel impairment-aware RMSA scheme to increase spectral efficiency while reducing the power consumption of an EON.

By accurately accounting for impairments in real-time, our scheme mitigates the limitations associated with fixed-guard band and fixed-transmission reach approaches while offering a higher spectral efficiency. For each traffic connection, the RMSA is performed only once and no disruptions (e.g. re-routing) are caused in the future. With efficient use of available spectrum, our scheme enables a service provider to accommodate more traffic with ease especially during peak hours. Moreover, by routing traffic carefully, our scheme identifies and turns off links, thereby reducing power consumption. The main contributions of this paper are as follows. We;

- Adopt an accurate noise model to estimate impairments experienced by each incoming traffic connection;
- Formulate a route selection criterion, which enables traffic to be accommodated using fewer links;
- Propose an Integer Linear Programming (ILP) formulation to jointly optimize spectral efficiency and power consumption of small networks;
- Propose a heuristic RMSA algorithm to jointly optimize spectral efficiency and power consumption of large networks under dynamic traffic environments; and
- Provide the flexibility to fine-tune our heuristic to achieve maximum spectral efficiency, minimum power consumption, or balanced performance.

The organization of this paper is as follows. Section II summarizes related work. Section III presents the network model, the PLI model, and the power consumption model. The proposed RMSA scheme including the ILP formulation and the heuristic are presented in Section IV. Section V presents and discusses the numerical results. Finally, Section VI concludes the paper.

II. RELATED WORK

In the evolution of optical transport networks, flexible-grid EONs have been identified as the next major breakthrough [34]. Thus, a larger number of researchers have dedicated their time and effort to rectify any issues that may arise as the transition from fixed-grid WDM to EONs takes place [34]–[36]. They have discussed possible methods of mitigating the unbearable CAPEX while maintaining service stability. To increase network throughput and reduce traffic blocking in EONs, advanced resource allocation (RA) schemes have been proposed by researchers for both long-haul (i.e., backbone) [7], [8], [16], [37] and short-haul (i.e., access and data-center) networks [38]–[40]. CAPEX and OPEX minimization have also been explored in a number of studies [2], [12], [18], [19]. As impairments have shown to hinder the performance of an EON, many researchers have proposed PLI-aware resource allocation schemes as well [7], [8], [16]. In this section, we provide a summary of this important literature and explain the motivation for our work.

A. SPECTRUM-AWARE RA SCHEMES

In general, the resource allocation schemes for EONs have been developed in the form of an analytical formulation (ILP) or a heuristic. The objective of these proposed schemes has often been to either increase spectral efficiency or reduce power consumption. Higher spectral efficiency and better utilization of available network resources lead to less traffic blocking, more useful bandwidth, and lower power consumption.

In 2010, Christodoulopoulos *et al.* analyzed the performance of several RA algorithms in EONs [25]. Here, the authors primarily focused on the static RA problem. Their results indicate that traffic connection sorting plays a critical role in spectral efficiency gains. The geometric optimization-based RA scheme proposed in [24] has explored three routing and three traffic ordering procedures and compares them in terms of total transmitted power. In [26], Velinska *et al.* presented two strategies to minimize the utilized spectrum and maximize the number of allocated connection requests. The first strategy allocates dynamic traffic according to the shortest paths and the second strategy is based on a genetic algorithm. Wang *et al.* proposed an algorithm that solves the routing and spectrum allocation (RSA) problem of a translucent (i.e., a network with re-generators) EON in a short time [27]. In 2016, Klinkowski *et al.* also proposed a novel routing, spectrum, transceiver, and regeneration allocation scheme for translucent networks [28]. However, the aforementioned algorithms often over-provision network resources [24]–[28] as many of them did not use an accurate impairment model, relied on fixed guard bands and simplified transmission reach models, which depend on worst-case network performance.

With the advent of accurate noise models, several impairment-aware resource allocation schemes came into existence in the last decade. Various research groups took different approaches and proposed ILP-based solutions, heuristic algorithms, and Artificial Intelligence (AI) based algorithms. In [7] and [41], Zhao *et al.* proposed a novel PLI-aware RMSA scheme for EONs with static traffic. The authors demonstrated the benefit of using an actual impairment model by comparing the spectral efficiency results against fixed-guard band approaches. Following the same principle, multiple RA schemes were then developed in [42]–[47] to increase spectral efficiency in static and dynamic EONs. In these work, novel power and code rate assignment techniques, traffic grooming, multi-path routing,

and regenerator placement algorithms were proposed to further increase spectral efficiency. In the work proposed in [48], four different spectrum assignment techniques (first fit, longest path first, most sub-carrier first, and pairwise farthest spectral distance (PFSD)) were evaluated through extensive simulations. Their results show that the PFSD scheme performs well in terms of noise tolerance over the other three spectrum assignment techniques without requiring additional hardware.

In 2019, Behera et. al proposed a novel impairment-aware routing, bit-loading, and spectrum allocation algorithm, which ensures a minimum end-to-end bit error rate (BER) for each demand [8]. After sorting traffic according to bandwidth requirements, the connections are served sequentially assuming each connection encountered the worst-case traffic congestion. In [49], the authors presented an online-offline probabilistic routing, spectrum, and regeneration assignment algorithm. In their work, PLIs are estimated using the Probabilistic Spectrum Gaussian Noise model to obtain higher spectral efficiency over work that utilizes transmission reach models. Most recently, in [50], the researchers presented a dispersion-sensitive spectrum allocation scheme to suppress the call blocking ratio in EONs. This approach allocates lower dispersion effect spectrum slots to the longer light-path requests and higher dispersion effect spectrum slots to the shorter light-path requests.

The efforts pertaining to the use of AI and Machine learning in resource allocation is well-documented in [51]. In [52], the authors proposed a dynamic fuzzy-based algorithm for EONs that utilize multi-core fibers. In this study, resource utilization was increased by 12.5%, on average, by using a combination of various clustering techniques. In [53], a deep learning based routing and spectrum assignment strategy was proposed to reduce spectrum fragmentation and traffic blocking.

B. POWER-AWARE RA SCHEMES

The work in [32], [33], [54] and [55] minimize power consumption by switching off network nodes and links. While guaranteeing full network connectivity, these post-analysis methods switch off underutilized network resources. The post analysis method presented in [56] also tries to switch off resources by re-routing traffic. A mathematical model to exploit sleep mode operation in an Internet Service Provider's (ISP's) network while maintaining the quality of service was proposed by [57]. According to this approach, power-hungry links can be turned off by splitting traffic over multiple paths. The work presented in [18] optimizes the backup resources according to the actual bandwidth requirement and reduces power consumption by 27%.

In [29] and [30], the authors presented a mixed ILP that jointly considers the assignment of modulation formats and optical grooming with the objective of minimizing energy consumption. The heuristic presented in [31] identified and adopted the routing path with the lowest energy consumption value. It outperforms the traditional shortest path and minimum hop-count algorithms in terms of energy saving.

In [58], the authors placed a re-generator at the most energy efficient position when quality of transmission (QoT) constraints of traffic connections are not met. The work in [37] proposed a distance-adaptive energy-aware RA scheme to increase spectral efficiency and, thereby, reduce the energy consumption of a survivable space division multiplexed EON.

Although these available schemes indicate good power conservation capabilities, their real-life applicability is hindered by several limitations. First, the majority of this work has not measured the actual linear and nonlinear PLI that would vary according to the present status of the network. Instead, these schemes rely on fixed guard-bands and preassigned maximum transmission distances, which will result in excess spectrum use [7]. Second, the use of a post-analysis method could cause disruptions to existing connections and induce quality issues. Third, the primary objective of most prior work is reducing power consumption and, therefore, very little consideration is afforded to bandwidth efficiency. Fourth, only a few studies have compared the performance of their proposed heuristic against an optimal solution (i.e., ILP). Moreover, to the best of our knowledge, no existing scheme accurately accounts for impairments and can jointly optimize spectral efficiency and power consumption. To address these limitations, in this paper, we propose a novel impairment-aware RMSA scheme that jointly optimizes spectral efficiency and the power consumption of an EON, while accurately accounting for its impairments. Figure 1 provides an overview of how spectral efficiency and power consumption is expected to vary when a network is optimized with spectrum-aware, power-aware, and our proposed schemes.

III. NETWORK MODEL AND PARAMETERS

The networks in this study are modelled in the form of a graph, which has N number of nodes and E number of edges (i.e., links). Each node communicates with every other node; hence, they act as both source nodes and destination nodes. The total bandwidth of each unidirectional link (i.e., a single-core optical fiber) is divided into F_{max} number of sub-carriers with each having a bandwidth of ζ. Depending on the physical length, link l is divided into N_l number of spans. Each span has a length of L, and is accompanied by an optical amplifier (OA) [18]. B_i represents the number of sub-carriers used by connection i (i.e., a traffic flow) between a node pair. The bandwidth of connection i is $B_i \times \zeta$. The connection i can be routed on one of the k different candidate paths in R_i, where $R_i = \{r_1, r_2, \ldots, r_k\}$. Path $r \in R_i$ may traverse through one or more links and link l can be along path r. Every node is employed with bandwidth-variable transponders that can transmit and receive connections modulated at $|M|$ different levels [7], [8].

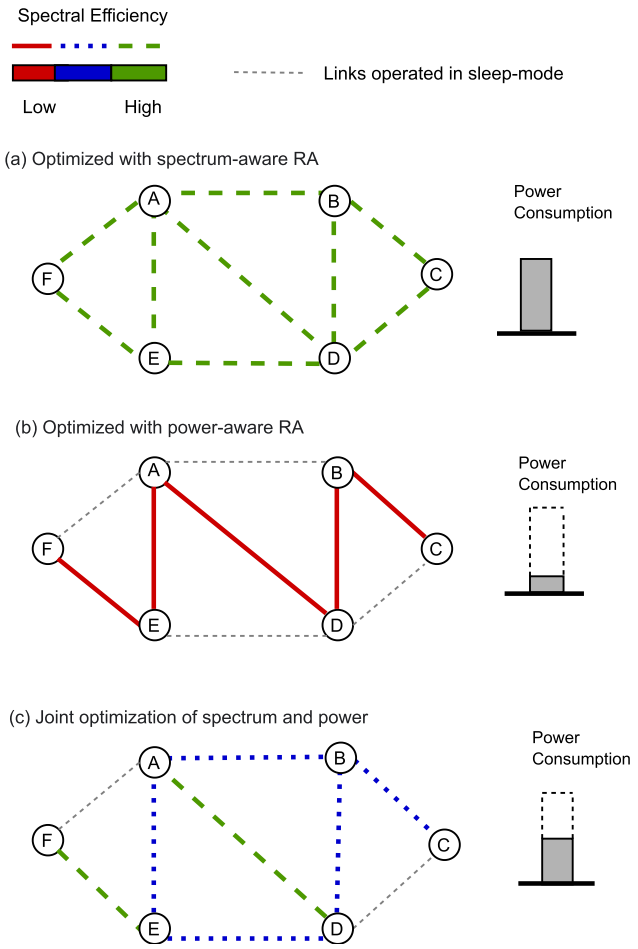

FIGURE 1. Spectral efficiency and the power consumption of a simple 6 node network optimized with three different RA schemes. In here, (a) offers the best spectral efficiency at the cost of highest power consumption, (b) consumes the least power but has a very low spectral efficiency, and (c) provides a balance between spectral efficiency and power consumption.

A. PLI MODEL

The PLI model used in this study is based on the GN model, which was first presented in [59] and was later adopted in several other work [16], [17], [46], [60]. The GN model accurately accounts for linear and non-linear impairments that are produced by amplified spontaneous emission (ASE), self-channel interference (SCI), and cross-channel interference (XCI). The signal-to-noise ratio (SNR) for connection i, can then be expressed as;

$$SNR_i = \frac{G}{G_{ASE} + G_{NLI}} \tag{1}$$

where, G, G_{ASE}, and G_{NLI} represent the power spectral densities (PSDs) of the signal, the ASE noise, and the noise from nonlinear impairments (NLI), respectively. When a connection i is modulated with format m where $m \in M$, the quality of transmission for the connection i is guaranteed if the condition $SNR_i \geq SNR_m$ is satisfied, where SNR_m represents the SNR threshold required to satisfy the bit error rate (BER) performance of the assigned modulation format. The detailed calculations are presented in the Appendix.

B. POWER CONSUMPTION MODEL

Several components contribute to the overall power consumption of the optical network. Among them, the Erbium-doped OAs that are placed along the optical fibers consume a significant amount of power, especially in large EONs [18]. Thus, the power consumed by link l_x that has a length of L_x can be calculated as;

$$P_{l_x} = \left\lfloor \frac{L_x}{L} \right\rfloor \times (P_{amp} + P_{fan}) \ [W]. \tag{2}$$

where P_{l_x} is the power consumed by link l_x, P_{amp} is the power consumed by an OA module, and P_{fan} is the power consumed by the control circuitry, power supply, and fan unit.

IV. PROPOSED RESOURCE ALLOCATION SCHEME

This section first defines the problem and then elaborates the proposed solution(s). The objective of this study is to develop a novel impairment-aware RMSA scheme that provides high spectral efficiency and reduced power consumption. The problem is thus defined as follows:

Given: the network parameters and QoT constraints (satisfy the SNR condition defined in Section III-A), develop an online RMSA scheme to,

Minimize: **(A)** Bandwidth waste
(B) Power consumption of the network

While adhering to: continuity, contiguity, non-overlapping spectrum allocation and QoT constraints.

In this study, bandwidth waste is quantified in terms of the highest sub-carrier index F_M assigned to any connection on any link [7]. Here, the power consumption is minimized by turning off a large number of links in the network and attached OAs. While parameters such as the code rate and power levels [24], [61] can also be optimized to achieve the desired objective (i.e., (A) and (B)), the proposed solution in this paper is limited to a novel RMSA scheme only.

A. ILP-BASED RMSA SCHEME FOR SMALL NETWORKS

With the objective of jointly minimizing bandwidth waste and power consumption of the EON, the problem can be mathematically expressed as the proposed ILP. In this study, F_N and X_N are the two optimization variables. Here, F_N is the normalized value of the maximum allocated sub-carrier index of the network, which is taken as the measure of spectral efficiency [7]. Variable X_N is the normalized value of the total number of active links in the network, which is directly proportional to the power consumption of the network.

The normalized value, F_N, is obtained by dividing the maximum allocated sub-carrier index of the network (F_M) by the largest sub-carrier index of the network (F_{max}). By carefully assigning the spectrum slots, the proposed scheme minimizes the maximum sub-carrier index on any link, which in turn, saves precious bandwidth and serves more traffic connections. The normalized value, X_N, is obtained by

TABLE 1. Input parameters and variables of the developed ILP.

Symbol	Definition
ILP Input Parameters	
$z_{ln} \in \mathbb{B} = 0, 1$	z_{ln} = 1 if node n is the end node of link l
$v_{in} \in \mathbb{B}$	v_{in} = 1 if n is the source or the destination of con. i
$T_{im} \in \mathbb{N}$	Number of sub-carriers of con. i when modulated with modulation format m
J^{ct}_{imh}	The partial NLI introduced by connection i on another connection when i is assigned modulation format m and the center frequency spacing between them is $h\zeta/2$ where $h \in \mathbb{N}$ denotes the number of sub-carrier half bandwidths (Appendix A)
H^{NLI}_{im}	The partial NLI of connection i when it is assigned modulation format m (Appendix A)
$\Theta \in \mathbb{N}$	A large number
ILP Input Variables	
$i \in \mathbb{N}$	The connection request considered
$j \in \mathbb{N}$	A previously allocated connection request where $j \neq i$
$m \in \mathbb{N}$	The modulation format considered
$l \in \mathbb{N}$	The link considered
$h \in \mathbb{N}$	The number of sub-carrier half-bandwidths
$\delta_1 \in \mathbb{R}$	The weight parameter used in the objective function
$F_M \in \mathbb{N}$	Maximum allocated sub-carrier index of the network
$F_N \in \mathbb{R}$	The normalized maximum allocated sub-carrier index of the network where $F_N = F_M/F_{max}$
$F_{max} \in \mathbb{N}$	The total number of sub-carriers in one link
$X_M \in \mathbb{N}$	The total number of active links in the network
$X_N \in \mathbb{R}$	The normalized value of X_M where $X_N = X_M/E$
$B_i \in \mathbb{N}$	The number of sub-carriers required for con. i
$f_i \in \mathbb{N}$	The lowest sub-carrier index (first sub-carrier index) allocated to con. i
$p^{link}_{il} \in \mathbb{B}$	p^{link}_{il} = 1 if link l is on the route assigned to con. i
$p^{node}_{in} \in \mathbb{B}$	p^{node}_{in} = 1 if node n is on the route assigned to con. i
$M^{mod}_{im} \in \mathbb{B}$	M^{mod}_{im} = 1 if con. i is assigned modulation format m
$y^{share}_{ij} \in \mathbb{B}$	y^{share}_{ij} = 1 if con. i and con. j share at least one common link
$u^{share}_{ij} \in \mathbb{B}$	u^{share}_{ij} = 1 if y^{share}_{ij} = 1 and $f_i + B_i \leq f_j$
$\Delta^{(h)}_{ijm} \in \mathbb{B}$	$\Delta^{(h)}_{ijm}$ = 1 if the center frequency spacing between con. i and j is $h\zeta/2$ and M^{mod}_{jm} = 1
$w^{ct}_{ijl} \in \mathbb{R} \leq 0$	Upper bound of the NLI on con. i from con. j in link l
$t^{NLI}_{il} \in \mathbb{R} \leq 0$	Upper bound of G^l_{NLI} of con. i on link l
$q^{route}_{ir} \in \mathbb{B}$	q^{route}_{ir} = 1 if con. i is routed along path r
$x_i \in \mathbb{N}$	Number of new active links required for each connection

dividing the number of active links (i.e., links that carry traffic) in the network (X_M) by the total number of links in the network (E). By accommodating an incoming connection via already active links, the proposed scheme always tries to minimize X_N when serving traffic.

Since normalized values are used for two optimization variables, they carry equal weight. However, δ_1 is introduced into the equation to tilt the balance towards one objective if needed. In the ILP, we have assigned $\delta_1 = 0.5$ to provide equal priority to the two optimization variables. For clarity, all the parameters and variables relevant to the ILP are expressed in Table 1.

$$\textbf{\textit{Minimize}}\ \delta_1 F_N + (1-\delta_1)X_N \tag{3}$$

$$\textbf{Subject to}: \Sigma_m M^{mod}_{im} = 1 \quad \forall i \tag{4}$$

$$\Sigma_r q^{route}_{ir} = 1 \quad \forall i \tag{5}$$

$$B_i = \Sigma_m T_{im} M^{mod}_{im} \quad \forall i \tag{6}$$

$$F_M \geq f_i + B_i - 1 \quad \forall i \tag{7}$$

$$\Sigma_l\, p^{link}_{il} z_{ln} = 2\, p^{node}_{in} - v_{in} \quad \forall i, n \tag{8}$$

$$p^{link}_{il} + p^{link}_{jl} \leq 1 + y^{share}_{ij} \quad \forall i, j \neq i, l \tag{9}$$

$$f_i + B_i - f_j \leq \Theta\,(1 - u^{share}_{ij}) \quad \forall i, j \neq i \tag{10}$$

$$f_j + B_j - f_i \leq \Theta\,(1 - y^{share}_{ij} + u^{share}_{ij})\ \forall i, j \neq i \tag{11}$$

$$x_i = \Sigma_l (P^{link}_{il} - y^{share}_{ij}) \quad \forall i, j \neq i \tag{12}$$

$$X_M \geq \Sigma_i x_i \quad \forall i \tag{13}$$

$$G\ \Sigma_m M^{mod}_{im}/SNR_m \geq G^0_{ASE}\Sigma_l P^{link}_{il} N_l + \Sigma_l N_l t^{NLI}_{il} \quad \forall i \tag{14}$$

$$t^{NLI}_{il} \geq \Theta\,(p^{link}_{il} - 1) + \Sigma_m M^{mod}_{im} H^{NLI}_{im} + \Sigma_{j \neq i} w^{ct}_{ijl} \quad \forall i, l \tag{15}$$

$$w^{ct}_{i,j,l} \geq \Theta(p^{link}_{i,l} - 1) + \Sigma_{m,h} \Delta^{(h)}_{ijm} J^{ct}_{jmh} \quad \forall i, j \neq i, l \tag{16}$$

$$\Sigma_h \Delta^{(h)}_{ijm} = M^{mod}_{jm} \quad \forall i, j \neq i, m \tag{17}$$

$$\Sigma_{m,h} h \Delta^{(h)}_{ijm} \leq \Theta(1 - u^{share}_{ij}) + 2(f_i - 1) + B_j - 2(f_i - 1) - B_i \quad \forall i, j \neq i \tag{18}$$

$$\Sigma_{m,h} h \Delta^{(h)}_{ijm} \leq \Theta(1 - y^{share}_{ij} + u^{share}_{ij}) + 2(f_i - 1) + B_i - 2(f_i - 1) - B_j \quad \forall i, j \neq i \tag{19}$$

The set of constraints in the ILP can be interpreted as follows: (4) and (5) of the ILP ensure that only one modulation format and only one route is assigned to each connection; (6) implies that the number of sub-carriers required for connection i (i.e., B_i) depends upon the modulation format selected; (7) ensures that for each connection, i, the last allocated sub-carrier index (i.e., $f_i + B_i - 1$) does not exceed the maximum allocated sub-carrier index of the network (i.e, F_N); (8) ensures that the route assigned to each i should be a no-looped route; (9) highlights that the value of y^{share}_{ij} is equal to one if connections i and j share at least one common link and, in such situations, (10) and (11) ensure that the spectrum allocated to the two connections on the shared link does not overlap. Equations (12) and (13) count the number of new links added to the network by each connection for each route.

Equations (14) to (19) ensure the satisfaction of the SNR requirement of each connection considering the PSDs of ASE noise and NLI. In the process of satisfying the SNR requirement for connection i, (14) considers the PSDs of ASE noise

and NLI while (15) determines the NLI PSD of connection i on link l and (16) determines the NLI PSD from connection j to connection i on link l. Equation (17) bounds the value of $\Sigma_h \Delta_{ijm}^{(h)}$ to 1 when connection j is assigned m while (18) and (19) ensure that $\Sigma_h \Delta_{ijm}^{(h)}$ is no larger than the central frequency spacing between connections i and j, accounting for the cases where connection i is placed in a lower or higher frequency band than j.

The number of variables and constraints in the ILP formulation depends on the number of connection requests I, the number of links E, the number of routes R, the number of nodes N in the network, the number of sub-carriers on each link S, and the number of total modulation formats M. Thus, $2I$+E+1 integer variables, $2I^2 + I^2MS + IE + IN + IM + IR$ Boolean variables, $I^2E + IE$ real variables, $2I+IN+I^2+I^2M$ Boolean equality constraints, I^2E Boolean inequality constraints, I integer equality constraints, $I + 5I^2$ integer inequality constraints, and $I+IE+I^2E$ real inequality constraints are involved in the proposed ILP.

The complexity of the ILP is directly linked to the number of variables and constraints. The complexity of Integer variables, Boolean variables and real variables are $\mathcal{O}(|I|+|E|+1)$, $\mathcal{O}(|I|^2|M||S|+|I||E|)$, and $\mathcal{O}(|I|^2|E|)$, respectively. The complexity of Boolean equality constraints for (4), (5), (8), and (17) is $\mathcal{O}(|I|^2|M| + |I||N|)$, Boolean inequality constraints for (9) is $\mathcal{O}(|I|^2|E|)$, integer equality constraints for (6) and (12) is $\mathcal{O}(|I| + |I|^2)$, integer inequality constraints for (7), (10), (11), (13), (18) and (19) is $\mathcal{O}(|I|^2)$ and real inequality constraints for (14), (15) and (16) is $\mathcal{O}(|I|^2|E|)$. It is important to note that for a real-sized network, I, E, and N will take large values (e.g., DT network with 14 nodes and 46 links) and, therefore, the ILP will be complex and require longer computational time.

B. HEURISTIC ALGORITHM

Due to associated complexity, the proposed ILP is only feasible for a small-sized network with an offline traffic matrix. Therefore, a low complexity heuristic algorithm is proposed. The network to be optimized using the proposed heuristic algorithm is assumed to have the following characteristics:

- The connection requests between different source-destination pairs arrive sequentially at random intervals and stay infinitely.
- The connection requests are served in the corresponding order they arrive.
- Impairments due to switching at intermediate optical cross-connectors are assumed to be negligible compared to ASE and NLI.
- Spectral spacing (i.e., guardband) between co-propagating connections is adjusted dynamically by taking into account actual impairments and QoT constraints.

Before the resource allocation process begins, the maximum sub-carrier index of the network, F_M, is set to a small value (e.g. $F_M = 20$). For a given connection request, i, between any node pair, k shortest paths are pre-calculated and stored in R_i. Initially, all the links, E, are in link-off state ($X_M = 0$). As notation C_υ denotes the number of existing connections in the network, at the very beginning, $C_\upsilon = 0$. The notations used in the proposed algorithm are summarized in Table 2. The relevant equations for PLI calculations are defined separately in Section IV-B2.

TABLE 2. Parameters and variables used in the proposed heuristic algorithm.

Symbol	Description
M	Set of modulation formats; $M = \{m_1, ..., m_M\}$
m_1	Highest order modulation format
f_i	First sub-carrier Index allocated to connection i
R_i	Set of shortest possible paths for i $(R_i = r_1, r_2, ..., r_k)$
r_1	The shortest path
S_r^m	Set of available continuous and contiguous slots along r
b_x	An item in S_{ir} where $len\,(b_x = T_{im})$
x	$x \in \mathbb{N}$
C_l	Cost of link l
F_l	Maximum allocated sub-carrier index of the link l
F_M	Maximum allocated sub-carrier index of the network
F_{max}	Total number of sub-carriers in one link
X_M	Total number of the active links in the network
W_l	Number of connections served along l
C_υ	The connection count of the network
N_r^0	Number of links along with no previously served traffic

When a connection request i arrives at the network, Algorithm Part 1 (AP1) is initiated. The current network status ($\bar{N}$), current link status ($\bar{E}$), current F_M value ($\bar{F_M}$), current X_M value ($\bar{X_M}$), and R_i are provided as inputs to AP1. The primary task of AP1 is to identify the modulation format and spectrum that satisfy the *SNR* requirements and, thus, can be used to route connection i along every $r \in R_i$.

For the first route $r \in R_i$, the algorithm starts exploring the available modulation formats. For a considered modulation format, $m \in M$, T_{im} is calculated. Next, from the available contiguous and continuous spectrum along the links of route r, every set, b_x, that has a length equal to T_{im} (e.g. $|b_x| = T_{im}$) is stored in S_r^m (e.g. $S_r^m = b_1, b_2, \ldots, b_x$). Note that the entries in S_r^m are sorted in ascending order of the slot numbers.

The algorithm now finds out if connection i can be accommodated using the modulation format m and spectrum slots, b_x. If Conditions (1) and (2) defined in Section IV-B2, which account for impairments, are satisfied, the chosen $\{CON : i, MOD : m, ROUTE : r, SLOT : b_x\}$ are stored as an entry within Ψ_i and the process repeats for the next route in R_i. However, if a feasible modulation format or spectrum cannot be found on route $r \in R_i$, then the F_M value is increased by 1 and the search process is repeated. At the end of AP1, Ψ_i will have k number of separate entries, where each entry will correspond to a route $r \in R_i$.

Once Ψ_i is defined, Algorithm Part 2 (AP2) is initiated. Here, each entry in Ψ_i is extracted separately. Depending on the *ROUTE*, $\bar{N}$, $\bar{E}$ of the entry, W_l is calculated for each l along the path defined by *ROUTE*. Notation N_r^0 accounts for

Algorithm Part 1 Finding the Modulation Format and Spectrum for Every $r \in R_i$

Inputs: $\bar{N}, \bar{E}, \bar{F_M}, \bar{X_M}, i, R_i, m$
Outputs: Ψ_i
for r in R_i **do**
  for m in M **do**
    Find T_{im}
    Find S_r^m ▷ $S_r^m = \{b_1, \ldots, b_x\}$ where $len(b_x) = T_{im}$
    Sort S_{ir}^m ▷ from lowest to highest sub-carrier index
    if $S_{ir}^m \neq \{\}$ **then**
      for b_x in S_{ir}^m **do**
        Temporarily allocate connection i
        for link l along r **do**
          Calculate C_l using Equation (21)
        end for
        Check Condition (1) and (2)
        if Satisfied **then** ▷ possible m and b_x are found
          Store $i, m, r, l \in r$ and b_x as $\psi = \{$ CON: i, MOD: m, ROUTE: r, SLOT: $b_x\}$
          Append ψ into Ψ_i
          Remove the temporarily allocated i
          Move to next $r \in R_i$ ▷ jump to Line: 4
        else: Continue ▷ try the next $b_x \in S_r^m$
        end if
      end for ▷ stop searching for the other b_x
      if No $b_x \in S_r^m$ satisfies Condition (1) and (2) **then**
        Try next $m \in M$ ▷ Jump to Line: 5
      else
        : Continue
      end if
    else ▷ $S_r^m = \{\}$
      Temporarily increase F_M by 1
      Jump to Line: 7 and re-do
    end if
  end for
end for

any link that does not carry any existing connections. Based on W_l and C_υ values, A_l is then calculated by dividing W_l by $(C_\upsilon - 1)$.

Here, A_l is the ratio between the number of existing connections on the selected link and the total connections in the network. A link that carries more connections will have a higher A_l value. Next, the normalized D_l is calculated by dividing the maximum used sub-carrier index of the particular link, F_l, by the maximum allocated sub-carrier index of the network, F_M.

For each link l in *ROUTE*, A_l values and D_l values are calculated through the above process and they are substituted into Equation (20) to find Y_R.

$$Y_R = \Sigma_{l \in r} \left(-\delta_2 A_l + (1 - \delta_2) D_l \right) \tag{20}$$

Here, δ_2 controls the weight of each parameter. Y_R along with N_r^0 and ψ are then appended as a candidate into Z_i. This process is repeated for all entities in Ψ_i. Among the candidates in Z_i, AP2 selects the candidate that has the smallest Y_R and lowest N_r^0 value and permanently allocates the connection i.

Algorithm Part 2 Finding the Best Route Among $r \in R_i$ to Accommodate Connection i

Inputs: $\bar{N}, \bar{E}, \bar{F_M}, \bar{X_M}, \Psi i, C_\upsilon, \delta_2, \theta_2$
Outputs: Accommodate connection i
Set: $N_r^0 = 0$
for ψ in Ψ_i **do** ▷ each entry in Ψ_i
  Retrieve *ROUTE* from Φ_i ▷ r in *ROUTE*
  for l in r **do** ▷ links along route r
    Find W_l ▷ number of existing connections along l
    if $W_l = 0$ **then** ▷ no existing connections along l
      Increase N_r^0 by 1
    else Continue:
    end if
    Calculate A_l ▷ $A_l = W_l/(C_\upsilon - 1)$
    Find F_l ▷ Maximum used sub-carrier index of l
    Calculate D_l ▷ $D_l = F_l/F_M$
    $Y_R += \left(-\delta_2 A_l + (1\text{-}\delta_2) D_l\right)$ ▷ Equation (20)
  end for
  Append $\{ Y_r, N_r^0, \psi \}$ into Z_i
end for
Sort Z_i in ascending order of Y_r value or N_r^0 value
Find the entry with non-zero N_r^0 and minimum Y_R of sorted Z_i
Extract i, r, m and b_x
Permanently assign i ▷ RMS are found for i to minimize F_M and X_M

1) RATIONALE FOR SELECTION OF THE CANDIDATE IN Z_i WITH THE SMALLEST Y_R AND LOWEST N_r^0

A higher A_l value indicates that the link is utilized by many existing connections. A lower D_l value indicates that the maximum sub-carrier index of that link is small compared to the largest sub-carrier index of the network. Therefore, the candidate with the smallest Y_R value can accommodate a connection using links that have a high utilization while keeping the maximum sub-carrier index low. A lower N_r^0 value indicates that a connection request can be accommodated using existing links without the need to activate new links. This can be understood well using the following example.

In the sample network shown in Figure 2, connection i is required to travel from node **A** to **C**. As $R_i = \{1 \rightarrow 2, 5 \rightarrow 4 \rightarrow 3, 6\}$, AP1 produces three separate entries for Ψ_i. The respective W_l and F_l values are indicated next

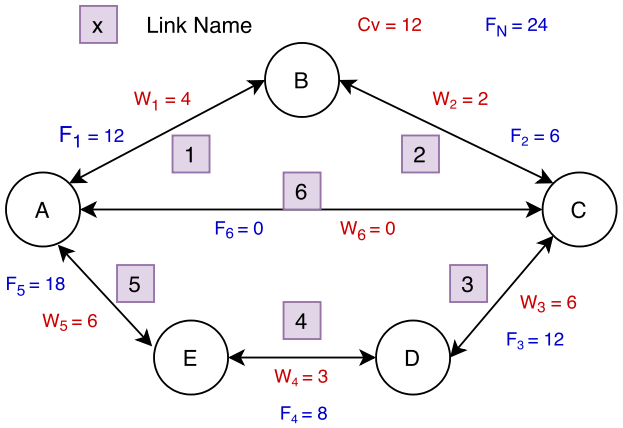

FIGURE 2. Example network.

TABLE 3. Calculation for Entry 1 in Ψ_i.

ROUTE	(1 → 2)	$\delta_2 = 0.5$
Link	1	2
A_l	4 / 12	2 / 12
D_l	12 / 24	6 / 24
$Y_{(1,2)}$	**0.126**	
$N^0_{(1,2)}$	**0**	

TABLE 4. Calculation for Entry 2 in Ψ_i.

ROUTE	(5 → 4 → 3)		$\delta_2 = 0.5$
Link	5	4	3
A_l	6 / 12	3 / 12	6 / 12
D_l	18 / 24	8 / 24	12 / 24
$Y_{(5,4,3)}$	**0.166**		
$N^0_{(5,4,3)}$	**0**		

to the links along the corresponding *ROUTE*. For this study, δ_2 is assumed to be 0.5 and the calculations are performed as shown in Tables 3, 4 and 5.

According to the calculation, the entry with the minimum Y_R and the minimum N^0_r is found to be ROUTE $(1 \rightarrow 2)$. Hence, the information in Entry 1 is used to serve the connection request.

2) PLI CALCULATION

The cost C_l in each link l is defined as;

$$C_l = N_l(G^0_{ASE} + \mu a \sinh(\rho\, T^2_{im}) + C^{past}_l + C^{future}_l) \quad (21)$$

In this equation, G^0_{ASE} is the PSD of ASE of a single span and its calculation is explained in the Appendix. Here, C^{past}_l is the partial NLI from each previously allocated connection j whose route includes link l, and it is calculated using Equation (22).

$$C^{past}_l = \mu\, \Sigma^{i-1}_{j=1} P^{link}_{jl}\, ln\Big[(\Delta f_{ij} + \frac{B_j}{2})/(\Delta f_{ij} - \frac{B_j}{2})\Big] \quad (22)$$

TABLE 5. Calculation for Entry 3 in Ψ_i.

ROUTE	(6)	$\delta_2 = 0.5$
Link	6	
A_l	0 / 12	
D_l	0 / 24	
$Y_{(6)}$	**0**	
$N^0_{(6)}$	**1**	

Further, C^{future}_l is the estimated NLI from Ξ future connections, and it is calculated using Equation (23). $X'_{eh'} = \mu \ln[1 + T_{e1}/(h' - T_{em_1}/2)]$ where h' is the smallest possible central frequency spacing between connection i and e with the assumption that the modulation format allocated to connection i is m', the first sub-carrier index allocated to connection i is f_i, and the modulation format for connection e is m_1; the highest one.

$$C^{future}_l = \Sigma^{i+\Xi}_{e=i+1}\, q'_{ei} X'_{eh'} \quad (23)$$

A route, a modulation format, and a range of continuous and contiguous spectrum slots can only be allocated for an incoming connection request i, if the following two conditions are satisfied:

- **Condition 1:** The *SNR* requirement for connection i when using the selected route should be;
  $\Sigma_{l \in r}\ C_l \leq G/SNR_m$
- **Condition 2:** The *SNR* requirement of each existing connection, j, is not violated after allocating connection i on the selected route with the selected modulation format and selected spectrum slots.

If the *SNR* requirements are not satisfied, the algorithm begins to sequentially explore:

- The next possible spectrum band on the selected route (i.e., b_x), and
- The next possible modulation format (i.e., m_2).

3) THE TRADE-OFF BETWEEN SPECTRUM AND POWER AND THE EFFECT OF δ_1 AND δ_2

The ILP and the heuristic are proposed to balance the trade-off between spectrum and power in EONs. Generally, an algorithm designed to reduce power consumption will compress all traffic into fewer fiber links, which in turn, will deplete spectral resources in those links leading to traffic blocking during peak hours. However, the proposed algorithm jointly optimizes power consumption and spectral efficiency to provide balanced performance. Thus, traffic connections will be tightly packed within the available spectral resources with minimal spacing among them as defined by the accurate impairment model. Even during peak hours, our proposed algorithm would then manage the available spectral resources more efficiently and, thus, inherently require fewer links. However, if traffic blocking is still present, the scheme will gradually activate more links. During

off-peak hours, as spectral resources are plenty, the proposed scheme will deactivate links to save power.

The weights δ_1 and δ_2 can be used to break this balance as required by the service provider. In short, by assigning a value over 0.5 to δ_1 and δ_2, service providers can achieve higher spectral efficiency. However, if a service provider's aim is to minimize power consumption, δ_1 and δ_2 values should be reduced accordingly. A balanced performance can be achieved by providing equal priority to these two objectives by assigning a value of 0.5 to both δ_1 and δ_2. To show how this trade-off will vary with respect to different weights, we have obtained results for different δ_2 values.

4) COMPLEXITY ANALYSIS OF THE HEURISTIC

As shown in the literature, the computation complexity of an algorithm can be analysed in terms of time complexity [8], [52]. To reduce time complexity, the proposed heuristic runs two separate algorithms (i.e., AP1 and AP2) in a sequence. To further reduce the time required to run AP1 and AP2, the k-shortest paths for traffic connections between each node pair are pre-calculated using an improved shortest-path algorithm proposed in [62] with a time complexity of $\mathcal{O}\left(|R|\,|N| + |E|\,log|N|\right)$ and are fed as inputs to the algorithm. The computational complexity of AP1 is bounded by $\mathcal{O}\left(|R|\,|M|\,|S|\,|I|\right)$, and the complexity of AP2 is bounded by $\mathcal{O}\left(|R|\,|E|\right)$ where R, M, S, E and I are the number of routes, the total number of modulation formats, the number of sub-carriers on each link, the number of links, and the number of connection requests, respectively.

V. PERFORMANCE EVALUATION

The performance of the proposed heuristic was evaluated by running numerical simulations on a randomly generated small 6-node network [7] with an average link length of 243 km and the realistic 14-node Deutsche Telekom (DT) network topology [14], [63], [64]. Spectral efficiency (measured in terms of the maximum sub-carrier index) and power consumption (calculated using the number of active links) were used as the two performance metrics.

The simulations were performed for varying network traffic loads. The network traffic was generated by randomly assigning a bit rate between 300 Gbps and 500 Gbps to each connection request. The value of F_{max} was taken as 320 and initial F_M was taken as 10. For every connection, resource allocation was performed by considering the three shortest paths ($k = 3$) and three modulation formats ($M = 3$). The three modulation formats used were $m_1 = 16$-QAM, $m_2 = 8$-QAM, and $m_3 = $ BPSK [8], [65]. The approximate SNR thresholds are 22.4 dB, 19.2 dB, and 12.6 dB, respectively, at BER 10^{-9} [8]. The physical parameters (indicated in the Appendix) were set to values: $\alpha = 0.22$ dB/km, $\gamma = 1.32(Wkm)^{-1}$, $\beta_2 = -21.7$ ps^2/km, $n_{sp} = 1.8$, $\nu = 193$ THz, $L = 80$ km, and $\zeta = 12.5$ GHz [1], [7], [29], [66].

Total network traffic was controlled by throttling the number of connection requests entering the network. At each network traffic load, the experiment was repeated multiple times and the average value was taken. Each connection had a random arrival time and an infinite resource holding time. A uniform power spectral density, $G = 20$ mW/THz, was considered, which according to previous work, gave the best results for the considered networks [7], [46]. The equations required to calculate the PSDs of the noise were directly adopted from Equations (2) and (4) of [7]. For power consumption calculations, $P_{amp} = 30$ W and $P_{fan} = 140$ W were adopted from [18] and [29].

A. HEURISTIC AGAINST THE ANALYTICAL MODEL

First, to gauge the performance and accuracy of the proposed heuristic, the results obtained for the small network were compared with the results of the proposed ILP and a First Fit (FF) spectrum allocation algorithm with a fixed guardband of 12.5 GHz [67], [68].

Spectrum allocation can be performed using the first-fit, random-fit and last-fit allocation policies [69]. Among these, fist-fit (FF) has often been used as a spectrum allocation strategy [8], [33], [40], [48], [50], [52], [58] and as a benchmark algorithm in previous studies [52], [70]. The FF is considered to be one of the best spectrum allocation policies as it packs connections into a smaller number of spectrum slots due to its lower call blocking probability and reduced computational complexity [69].

The FF policy maintains a list of available and used slots. In our study, FF serves an incoming connection by allocating the first available spectrum slots (i.e., lowest indexed slots) on a randomly selected path using the highest order modulation format [69]. The assigned slots are marked as used slots and the list is updated accordingly. By selecting spectrum in this manner, existing connections are packed into a smaller number of spectrum slots, leaving a large number of spectrum slots for future use in the selected path. However, FF does not explore all possible routing paths, modulation formats, and power consumption. Thus, obtaining a global minimum for spectrum allocation and power consumption is often difficult with FF [69].

The simulations were run on a desktop computer with 6-core, i7 8700 CPU and 32GB RAM. The typical running time for the ILP was 5 hours 30 minutes, and 58 minutes for the heuristic. The boundary between peak and off-peak traffic was drawn exactly at 40% of the maximum total traffic in plotted results [56].

Figures 3 and 4 depict the maximum sub-carrier index and the number of active links at each traffic load, respectively. The respective percentage performance improvement of each case with respect to the worst-case scenario is marked in every graph.

Based on the results depicted in Figure 3, it is observed that the maximum sub-carrier index increases as network traffic grows. Among the three algorithms, ILP offers the best results and, thus, requires the least bandwidth. The proposed low-complexity heuristic produces comparable results while consuming one-fifth of the running time. The FF algorithm consumes the most bandwidth at all traffic volumes.

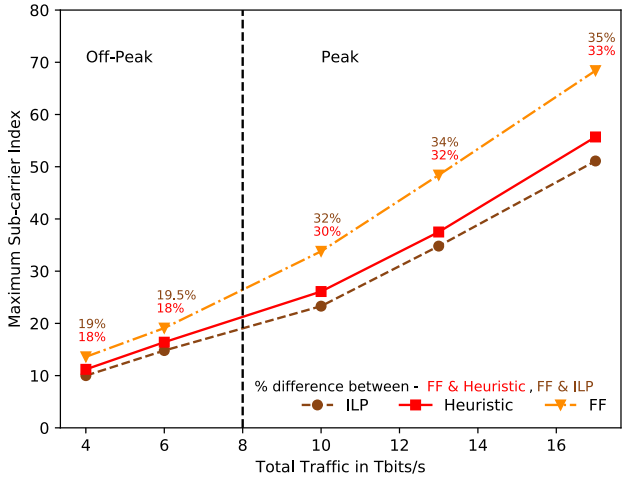

FIGURE 3. Maximum sub-carrier index of the ILP, the proposed heuristic, and the First Fit algorithm for the 6-node network (δ_1 and $\delta_2 = 0.5$).

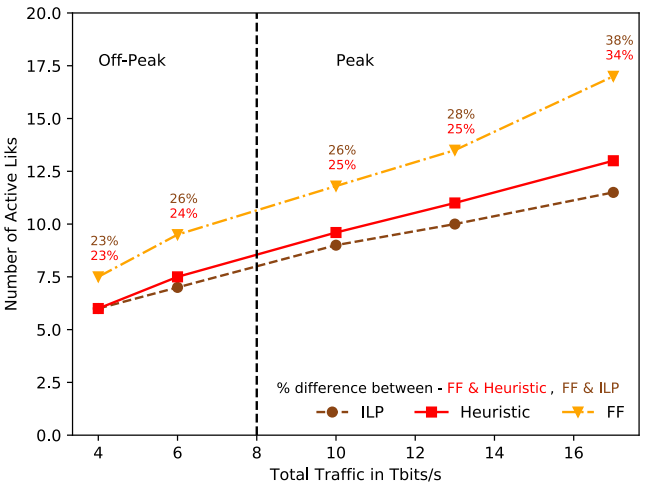

FIGURE 4. Number of active links with the ILP, the proposed heuristic, and the First Fit algorithm for the 6-node network (δ_1 and $\delta_2 = 0.5$).

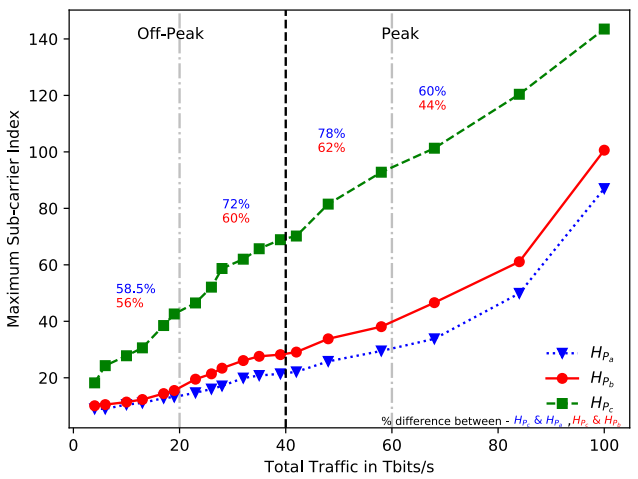

FIGURE 5. Maximum sub-carrier index of the three heuristics.

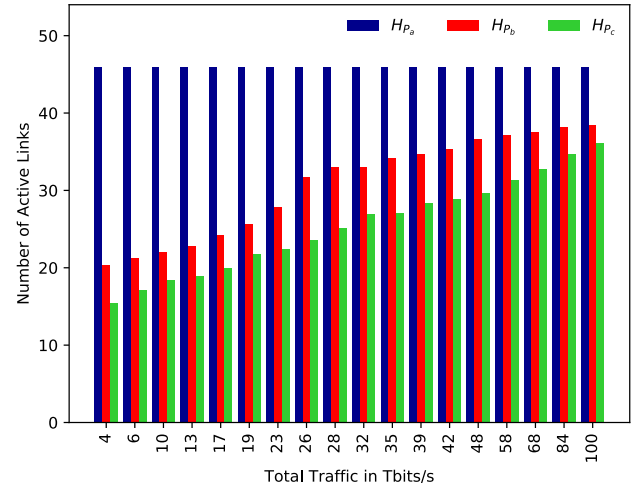

FIGURE 6. Number of active links with the three heuristics.

In Figure 4, the results show an increment in the number of active links with respect to growing traffic. This is an indication that more power is consumed at peak-traffic loads. Yet again, the ILP shows the best results and has fewer number of active links in the network at every traffic load. The results of the heuristic closely follow the ILP and requires 26.2% less active links over the FF algorithm.

B. RESULTS OBTAINED FOR THE DT NETWORK

For the large DT network, solving an ILP is impractical. Therefore, we have obtained the results using the heuristic. Initially, the heuristic was repeated for three different δ_2 values to compare the results of our joint optimization algorithm against power- and spectrum-aware algorithms.

1) $\delta_2 = 0$
This heuristic, denoted as H_{P_a}, is intended to increase spectral efficiency only (i.e., spectrum-aware RA scheme with an accurate noise model). It is similar to the impairment-aware algorithm presented in [7], which is often used as the benchmark in other researches as well [8], [16], [46].
2) $\delta_2 = 0.5$
This heuristic, denoted as H_{P_b}, gives equal weight to both performance metrics.
3) $\delta_2 = 1$
This heuristic, denoted as H_{P_c}, is intended to reduce power consumption only (i.e., power-aware RA scheme with an accurate noise model).

In Figure 5, the maximum sub-carrier index is plotted against the network traffic for the three heuristics. The results indicate that H_{P_c} consumes the most sub-carriers while H_{P_a} consumes the least. The difference between H_{P_a} and H_{P_c} is minimal ($< 8\%$) and, thus, both heuristics produce nearly identical results. A rapid increment in sub-carriers is observed when network traffic exceeds 60 Tbits/s.

Figure 6 shows the number of links in sleep and active states at different traffic loads for the three heuristics. Since

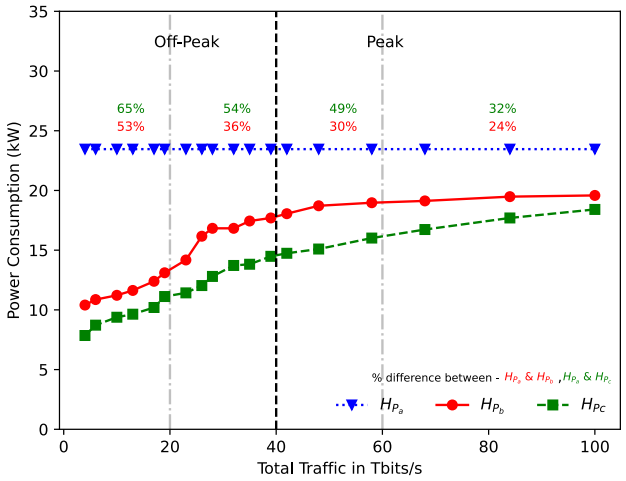

FIGURE 7. Power consumption of the three heuristics.

TABLE 6. Percentage increment in maximum sub-carrier index and number of links.

Parameter	Comparison	Average Difference
Maximum sub-carrier index	H_{P_b} vs H_{P_a}	11.63%
Number of active links	H_{P_b} vs H_{P_c}	14.36%

H_{P_c} is designed to minimize the number of active links, it gives the best result. The H_{P_b} closely follows the results of H_{P_c}, while H_{P_a} has all the links in the active state at all traffic loads.

Figure 7 shows the power consumption of the three heuristics under increasing traffic load. According to the power consumption model described in Section III and [18], the number of active links is directly related to the power consumption of the network. Hence, H_{P_c} consumes the least power, which is closely followed by H_{P_b}. The heuristic H_{P_a} does not optimize the number of active links and, thus, consumes the most power.

Table 6 summarizes the average difference between the proposed heuristic (H_{P_b}) and the respective best case scenario for spectrum efficiency (H_{P_a}) and power saving (H_{P_c}). By analyzing the results of Figures 5, 6, and 7 together with the summary presented in Table 6, we arrive at the conclusion that H_{P_b} provides balanced performance by consuming fewer sub-carriers and using fewer links.

Figure 8 shows the actual values of the sub-carrier index savings and power savings achieved by performing RMSA for a given network with H_{P_b} heuristic. On average, H_{P_b} can reduce power consumption (with respect to spectrum-aware RA) and maximum sub-carrier index (with respect to power-aware RA) by 45% and 58%, respectively, during off-peak hours. Similarly, during peak hours, H_{P_b} can save up to 20% of power and reduce the maximum sub-carrier index by 53%, which leads to lower OPEX and less traffic blocking.

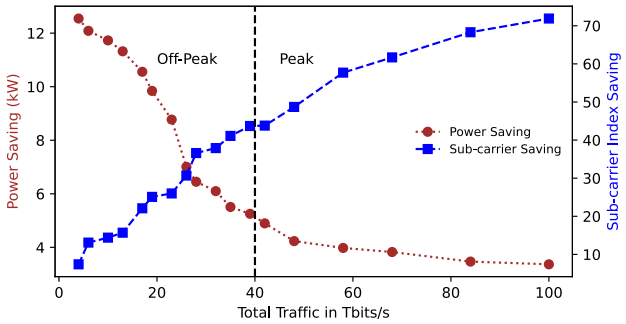

FIGURE 8. Sub-carrier and power savings with H_{P_b} heuristic.

C. RESULTS OBTAINED FOR DYNAMIC δ_2 ASSIGNMENT

Results in Figures 5 and 7 show that H_{P_a} ($\delta_2 = 1$) provides the highest spectral efficiency; yet it consumes the most power. On the other hand, H_{P_c} ($\delta_2 = 0$) consumes the least power at the cost of low spectral efficiency. The proposed H_{P_b} ($\delta_2 = 0.5$) provides a balanced performance. We now evaluate the performance improvements that can be obtained by dynamically adjusting δ_2 according to the traffic variation.

The spectral resources will not cause a bottleneck during off peak hours as the network will carry less traffic. Then the service providers (i.e., network operators) will divert their efforts to save more power by assigning a smaller value to δ_2, temporarily neglecting its effect on spectral efficiency. To maximize power savings, δ_2 can be assigned the value 0, as in H_{P_c}, during very low traffic periods. However, as traffic increases and moves gradually towards the peak, δ_2 can be adjusted accordingly to provide the best balance between spectral resources and power consumption. When the traffic reaches peak levels, spectral resources will become scarce and, therefore, δ_2 needs to be increased, as in H_{P_a}, and more links have to be activated. In Figure 9, we depict the percentage improvement in power consumption and spectral efficiency that can be obtained over H_{P_b} by dynamically adjusting δ_2. The results clearly indicate that by appropriately selecting δ_2 value, we can increase power savings during low traffic hours and spectral efficiency during heavy traffic hours, respectively.

D. IMPROVED HEURISTIC

Power consumption can be further reduced by turning off the longer links. To enable this, the multi-objective function formulated in Equation (20) has been modified by introducing an additional parameter Q_l. The modified objective function is presented in Equation (24), which is used to identify the path with minimum Y'_R for each and every connection request.

$$Y'_R = \Sigma_{l \in r} \left(-\delta_3 A_l + \theta_3 D_l + \Big(1 - (\delta_3 + \theta_3)\Big) Q_l \right) \quad (24)$$

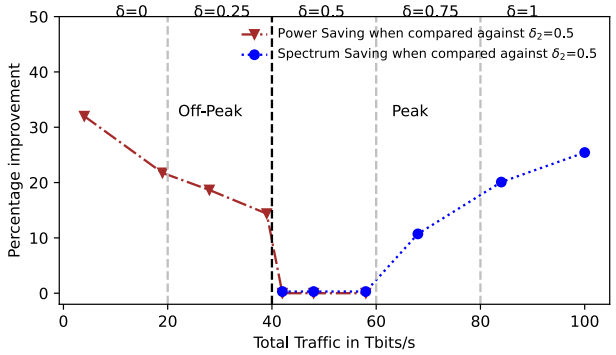

FIGURE 9. Percentage improvement of spectrum / power savings against H_{P_b} heuristic.

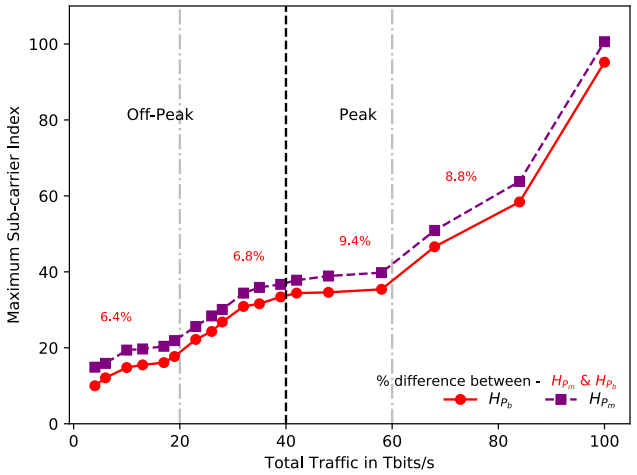

FIGURE 10. The maximum sub-carrier index of H_{P_m} and H_{P_b}.

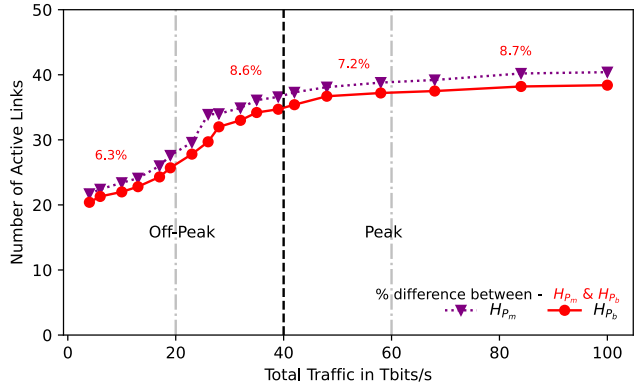

FIGURE 11. Number of active links of H_{P_m} and H_{P_b}.

For each link l, the Q_l is calculated by dividing the length of the considered link by the average link length of the network. The coefficients δ_3 and θ_3 are used as the regularization parameters. In this study, an equal priority is assigned to all three objectives and, thus, δ_3 and θ_3 have been assigned the value 0.33. The results obtained with this modified multi-objective function, named H_{P_m}, is compared against the results of H_{P_b} in Figure 10, 11, and 12.

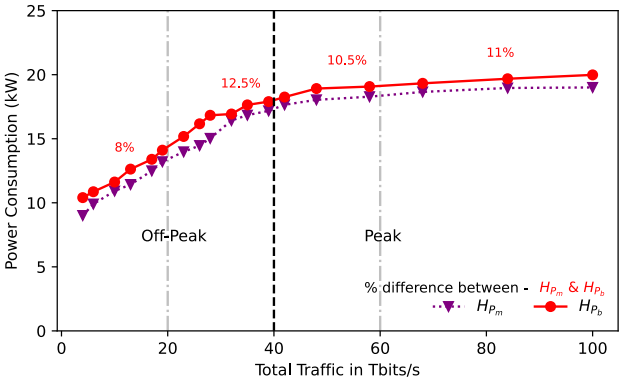

FIGURE 12. Power consumption of H_{P_m} and H_{P_b}.

These figures indicate that while H_{P_m} consumes slightly more (approximately 7.7%) sub-carriers and active links, it consumes less power.

By fine-tuning the weights assigned to the objective function, H_{P_m} RMSA scheme can be used by service providers to either increase spectral efficiency, thereby reducing traffic blocking, or to reduce the energy bill. On the other hand, by assigning equal weights to the coefficients, a balance between spectral efficiency and power saving can be maintained.

VI. CONCLUSION

In this paper, we developed an impairment-aware RMSA scheme that jointly optimizes the routing, modulation format, and spectrum per connection, thereby increasing spectral efficiency and reducing power consumption of an EON. Our proposed scheme accounts for actual linear and nonlinear impairments by monitoring the current status of the network. As resource allocation is performed to minimize spectrum use and power consumption at the entry point of every connection, the scheme causes zero disruptions to existing connections. By fine-tuning the weights of the coefficients, the scheme can be adjusted to attain the necessary balance between spectral efficiency and power consumption required by the service providers. Through numerical simulations, we demonstrated that the proposed heuristic offers similar results to the ILP, and, thus, can be used to optimize large networks with less complexity. Repeated tests indicate that by optimizing an EON with the proposed scheme, on average, spectral efficiency can be increased by 53% and power consumption can be reduced by 20% during peak hours.

APPENDIX A

The PSD of the amplified spontaneous emission (ASE) noise is $G_{ASE} = \Sigma_{l \in r} N_l G^0_{ASE}$ where $G^0_{ASE} = (e^{\alpha L} - 1)\, \eta_{sp} \hbar \nu$. Here, α is the power attenuation, η_{sp} is the spontaneous emission factor, $\hbar$ is Planck's constant and ν is the optical carrier frequency (light frequency).

The PSD of the noise from nonlinear impairments (NLI) is $G_{NLI} = \Sigma_{l \in r} N_l G^l_{NLI}$ where the PSD of the NLI noise in a

single span on link l G^l_{NLI} is;

$$G^l_{NLI} = \mu\left(ln\left(\rho B_i^2\right) + \sum_j ln\frac{\Delta f_{ij} + B_j/2}{\Delta f_{ij} - B_j/2}\right).$$

In this expression, $\mu = (3\gamma^2 G^3)/(2\pi\alpha|\beta_2|)$, $\rho = (\pi^2|\beta_2|)/\alpha$, γ is the fiber non-linearity coefficient, β_2 is the fiber dispersion and Δf_{ij} is the centre frequency spacing between connections i and j where i and j are two connections using link l. Interested readers may also refer to Equations (1), (2) and (4) of [7] for more information.

The partial NLI introduced by connection i on another connection, J^{ct}_{imh}, is calculated as: $J^{ct}_{imh} = \mu \ln \frac{h+T_{im}}{h-T_{im}} \in \mathbb{R} \geq 0$ where $h \in \mathbb{N}$ denotes the number of sub-carrier half bandwidths.

Similarly, H^{NLI}_{im} is calculated as: $H^{NLI}_{im} = \mu \ln(\rho(\zeta T_{im})^2) \in \mathbb{R} \geq 0$ where ζ is the bandwidth of each sub-carrier.

ACKNOWLEDGMENT

The authors extend their gratitude to Dr. Udaya Wijenayake for expert advice on the complexity analysis. They also thank the anonymous reviewers for their critical comments that greatly helped in improving the contents of this paper.

REFERENCES

[1] S. Liu, Q. Guo, J. Yuan, and Q. Zhang, "A resource-periodic-arrangement strategy for RMSA problem in elastic optical networks," *IEEE Access*, vol. 8, pp. 159745–159755, 2020.

[2] M. Zhu, Q. Sun, S. Zhang, P. Gao, B. Chen, and J. Gu, "Energy-aware virtual optical network embedding in sliceable-transponder-enabled elastic optical networks," *IEEE Access*, vol. 7, pp. 41897–41912, 2019.

[3] B. Yan, Y. Zhao, X. Yu, W. Wang, Y. Wu, Y. Wang, and J. Zhang, "Tidal-traffic-aware routing and spectrum allocation in elastic optical networks," *J. Opt. Commun. Netw.*, vol. 10, no. 11, pp. 832–842, 2018.

[4] B. C. Chatterjee, N. Sarma, and E. Oki, "Routing and spectrum allocation in elastic optical networks: A tutorial," *IEEE Commun. Surveys Tuts.*, vol. 17, no. 3, pp. 1775–1800, 3rd Quart., 2015.

[5] G. Zhang, M. De Leenheer, A. Morea, and B. Mukherjee, "A survey on OFDM-based elastic core optical networking," *IEEE Commun. Surveys Tuts.*, vol. 15, no. 1, pp. 65–87, 1st Quart., 2013.

[6] A. Ahad, M. Tahir, and K.-L.-A. Yau, "5G-based smart healthcare network: Architecture, taxonomy, challenges and future research directions," *IEEE Access*, vol. 7, pp. 100747–100762, 2019.

[7] J. Zhao, H. Wymeersch, and E. Agrell, "Nonlinear impairment-aware static resource allocation in elastic optical networks," *J. Lightw. Technol.*, vol. 33, no. 22, pp. 4554–4564, Nov. 15, 2015.

[8] S. Behera, A. Deb, G. Das, and B. Mukherjee, "Impairment aware routing, bit loading, and spectrum allocation in elastic optical networks," *J. Lightw. Technol.*, vol. 37, no. 13, pp. 3009–3020, Jul. 1, 2019.

[9] A. Napoli, M. Bohn, D. Rafique, A. Stavdas, N. Sambo, L. Poti, M. Nolle, J. K. Fischer, E. Riccardi, A. Pagano, A. Di Giglio, M. S. Moreolo, J. M. Fabrega, E. Hugues-Salas, G. Zervas, D. Simeonidou, P. Layec, A. D'Errico, T. Rahman, and J. P. F.-P. Gimenez, "Next generation elastic optical networks: The vision of the European research project IDEALIST," *IEEE Commun. Mag.*, vol. 53, no. 2, pp. 152–162, Feb. 2015.

[10] M. Jinno, "Elastic optical networking: Roles and benefits in beyond 100-Gb/s era," *J. Lightw. Technol.*, vol. 35, no. 5, pp. 1116–1124, Mar. 1, 2017.

[11] H. Ding, M. Zhang, B. Ramamurthy, Z. Liu, S. Huang, and X. Chen, "Routing, modulation level and spectrum allocation with dynamic modulation level conversion in elastic optical networks," *Photonic Netw. Commun.*, vol. 28, no. 3, pp. 295–305, Dec. 2014.

[12] K. Walkowiak, M. Woźniak, M. Klinkowski, and W. Kmiecik, "Optical networks for cost-efficient and scalable provisioning of big data traffic," *Int. J. Parallel, Emergent Distrib. Syst.*, vol. 30, no. 1, pp. 15–28, Jan. 2015.

[13] *Spectral Grids for WDM Applications: DWDM Frequency Grid*, document ITU-T G.694.1 (02/2012), 2012, pp. 1–16. [Online]. Available: http://www.itu.int/rec/T-REC-G.694.1/en%5Cnhttp://www.itu.int/rec/T-REC-G.694.1-201202-I/en

[14] K. Christodoulopoulos and E. Varvarigos, "Routing and spectrum allocation policies for time-varying traffic in flexible optical networks," in *Proc. 16th Int. Conf. Opt. Netw. Design Modeling (ONDM)*, Apr. 2012, pp. 1–6.

[15] X. Zhou, W. Lu, L. Gong, and Z. Zhu, "Dynamic RMSA in elastic optical networks with an adaptive genetic algorithm," in *Proc. IEEE Global Commun. Conf. (GLOBECOM)*, Dec. 2012, pp. 2912–2917.

[16] N. Dharmaweera, L. Yan, M. Karlsson, and E. Agrell, "An impairment-aware resource allocation scheme for dynamic elastic optical networks," in *Proc. Opt. Fiber Commun. Conf.*, 2017, paper Th2A.

[17] L. Lundberg, P. A. Andrekson, and M. Karlsson, "Power consumption analysis of hybrid EDFA/Raman amplifiers in long-haul transmission systems," *J. Lightw. Technol.*, vol. 35, no. 11, pp. 2132–2142, Jun. 1, 2017.

[18] J. Lopez, Y. Ye, V. Lopez, F. Jimenez, R. Duque, P. M. Krummrich, F. Musumeci, M. Tornatore, and A. Pattavina, "Traffic and power-aware protection scheme in elastic optical networks," in *Proc. 15th Int. Telecommun. Netw. Strategy Planning Symp. (NETWORKS)*, Oct. 2012, pp. 317–322.

[19] S. Aleksic and A. Lovric, "Power consumption of wired access network technologies," in *Proc. 7th Int. Symp. Commun. Syst., Netw. Digit. Signal Process. (CSNDSP)*, Jul. 2010, pp. 147–151.

[20] F. Musumeci, A. Hmaity, M. Tornatore, and A. Pattavina, "Energy efficiency in reliable optical core networks," in *Proc. IEEE Online Conf. Green Commun. (OnlineGreenComm)*, Nov. 2015, pp. 1–6.

[21] J. Baliga, R. Ayre, K. Hinton, and R. Tucker, "Energy consumption in wired and wireless access networks," *IEEE Commun. Mag.*, vol. 49, no. 6, pp. 70–77, Jun. 2011.

[22] R. S. Tucker, J. Baliga, R. Ayre, K. Hinton, and W. V. Sorin, "Energy consumption in IP networks," *J. Lightw. Technol.*, vol. 27, no. 13, pp. 2391–2403, Jul. 2009.

[23] M. N. Dharmaweera, R. Parthiban, and Y. A. Sekercioglu, "Toward a power-efficient backbone network: The state of research," *IEEE Commun. Surveys Tuts.*, vol. 17, no. 1, pp. 198–227, 1st Quart., 2015.

[24] M. Hadi and M. R. Pakravan, "Resource allocation for elastic optical networks using geometric optimization," *J. Opt. Commun. Netw.*, vol. 9, no. 10, pp. 889–899, Oct. 2017.

[25] K. Christodoulopoulos, I. Tomkos, and E. A. Varvarigos, "Routing and spectrum allocation in OFDM-based optical networks with elastic bandwidth allocation," in *Proc. IEEE Global Telecommun. Conf. (GLOBECOM)*, Dec. 2010, pp. 3111–3116.

[26] J. Velinska, I. Mishkovski, and M. Mirchev, "Routing, modulation and spectrum allocation in elastic optical networks," in *Proc. 26th Telecommun. Forum (TELFOR)*, Nov. 2018, pp. 907–910.

[27] X. Wang, M. Brandt-Pearce, and S. Subramaniam, "Impact of wavelength and modulation conversion on translucent elastic optical networks using MILP," *IEEE/OSA J. Opt. Commun. Netw.*, vol. 7, no. 7, pp. 644–655, Jul. 2015.

[28] M. Klinkowski and K. Walkowiak, "A heuristic algorithm for routing, spectrum, transceiver and regeneration allocation problem in elastic optical networks," in *Proc. 18th Int. Conf. Transparent Opt. Netw. (ICTON)*, Jul. 2016, pp. 1–4.

[29] Y. Tan, R. Gu, and Y. Ji, "Energy-efficient routing, modulation and spectrum allocation in elastic optical networks," *Opt. Fiber Technol.*, vol. 36, pp. 297–305, Jul. 2017.

[30] P. Biswas and A. Adhya, "Energy-efficient network planning and traffic provisioning in IP-over-elastic optical networks," *Optik*, vol. 185, pp. 1115–1133, May 2019.

[31] S. Y. M. Bandiri, T. C. Pimenta, and D. H. Spadoti, "Adaptive modulation and code strategy to reduce energy consumption in elastic optical network," *J. Microw., Optoelectronics Electromagn. Appl.*, vol. 17, no. 1, pp. 65–84, Mar. 2018.

[32] L. Chiaraviglio, M. Mellia, and F. Neri, "Minimizing ISP network energy cost: Formulation and solutions," *IEEE/ACM Trans. Netw.*, vol. 20, no. 2, pp. 463–476, Apr. 2012.

[33] G. Beletsioti, S. Mavridopoulos, G. Tziroglou, C. Kyriakopoulos, G. Papadimitriou, P. Nicopolitidis, and E. Varvarigos, "Power-aware algorithms for energy-efficient elastic optical backbone and metro networks," in *Proc. 16th Int. Joint Conf. e-Bus. Telecommun.*, 2019, pp. 69–76.

[34] R. Zhu, S. Li, P. Wang, Y. Tan, and J. Yuan, "Gradual migration of co-existing fixed/flexible optical networks for cloud-fog computing," *IEEE Access*, vol. 8, pp. 50637–50647, 2020.

[35] X. Chen, J. Li, B. Guo, P. Zhu, R. Tang, Z. Chen, and Y. He, "All-optical OXC transition strategy from WDM optical network to elastic optical network," *Opt. Exp.*, vol. 24, no. 4, pp. 4076–4087, Feb. 2016.
[36] X. Yu, M. Tornatore, M. Xia, J. Wang, J. Zhang, Y. Zhao, J. Zhang, and B. Mukherjee, "Migration from fixed grid to flexible grid in optical networks," *IEEE Commun. Mag.*, vol. 53, no. 2, pp. 34–43, Feb. 2015.
[37] R. Zhu, A. Samuel, P. Wang, S. Li, L. Li, P. Lv, and M. Xu, "Survival multipath energy-aware resource allocation in SDM-EONs during fluctuating traffic," *J. Lightw. Technol.*, vol. 39, no. 7, pp. 1900–1912, Apr. 1, 2021.
[38] H. Yang, X. Zhao, Q. Yao, A. Yu, J. Zhang, and Y. Ji, "Accurate fault location using deep neural evolution network in cloud data center interconnection," *IEEE Trans. Cloud Comput.*, early access, Feb. 17, 2020, doi: 10.1109/TCC.2020.2974466.
[39] H. Yang, Y. Liang, J. Yuan, Q. Yao, A. Yu, and J. Zhang, "Distributed blockchain-based trusted multidomain collaboration for mobile edge computing in 5G and beyond," *IEEE Trans. Ind. Informat.*, vol. 16, no. 11, pp. 7094–7104, Nov. 2020.
[40] H. Yang, J. Zhang, Y. Ji, R. Tian, J. Han, and Y. Lee, "Performance evaluation of multi-stratum resources integration based on network function virtualization in software defined elastic data center optical interconnect," *Opt. Exp.*, vol. 23, no. 24, pp. 31192–31205, Nov. 2015.
[41] J. Zhao, H. Wymeersch, and E. Agrell, "Nonlinear impairment aware resource allocation in elastic optical networks," in *Proc. Opt. Fiber Commun. Conf.*, 2015, paper M2I.1.
[42] M. N. Dharmaweera, L. Yan, M. Karlsson, and E. Agrell, "Nonlinear-impairments- and crosstalk-aware resource allocation schemes for multicore-fiber-based flexgrid networks," in *Proc. 42nd Eur. Conf. Opt. Commun. (ECOC)*, 2016, pp. 1223–1225.
[43] L. Yan, E. Agrell, H. Wymeersch, and M. Brandt-Pearce, "Resource allocation for flexible-grid optical networks with nonlinear channel model [invited]," *J. Opt. Commun. Netw.*, vol. 7, no. 11, pp. B101–B108, 2015.
[44] N. Dharmaweera, L. Yan, J. Zhao, M. Karlsson, and E. Agrell, "Regenerator site selection in impairment-aware elastic optical networks," in *Proc. Opt. Fiber Commun. Conf.*, 2016, pp. 6–8.
[45] M. N. Dharmaweera, J. Zhao, L. Yan, M. Karlsson, and E. Agrell, "Traffic-grooming-and multipath-routing-enabled impairment-aware elastic optical networks," *IEEE/OSA J. Opt. Commun. Netw.*, vol. 8, no. 2, pp. 58–70, Feb. 2016.
[46] K. Munasinghe, M. N. Dharmaweera, C. de Alwis, and U. Wijewardhana, "Novel impairment-aware resource allocation scheme for elastic optical networks serving traffic with different service priorities," in *Proc. 14th Conf. Ind. Inf. Syst. (ICIIS)*, Dec. 2019, pp. 308–313.
[47] J. Zhao, L. Yan, H. Wymeersch, and E. Agrell, "Code rate optimization in elastic optical networks," in *Proc. Eur. Conf. Opt. Commun. (ECOC)*, Sep. 2015, pp. 490–492.
[48] R. Krishnamurthy and T. Srinivas, "Physical layer impairments aware routing and spectrum allocation algorithm for transparent flexible-grid optical networks," *Comput. Commun.*, vol. 153, pp. 507–514, Mar. 2020.
[49] Y. Xu, E. Agrell, and M. Brandt-Pearce, "Cross-layer static resource provisioning for dynamic traffic in flexible grid optical networks," *IEEE/OSA J. Opt. Commun. Netw.*, vol. 13, no. 3, pp. 1–13, Mar. 2021.
[50] B. C. Chatterjee, N. Stol, and E. Oki, "Impairment-aware spectrum allocation in elastic optical networks: A dispersion-sensitive approach," *Opt. Fiber Technol.*, vol. 61, Jan. 2021, Art. no. 102431.
[51] Y. Zhang, J. Xin, X. Li, and S. Huang, "Overview on routing and resource allocation based machine learning in optical networks," *Opt. Fiber Technol.*, vol. 60, Dec. 2020, Art. no. 102355.
[52] H. Yang, Q. Yao, A. Yu, Y. Lee, and J. Zhang, "Resource assignment based on dynamic fuzzy clustering in elastic optical networks with multi-core fibers," *IEEE Trans. Commun.*, vol. 67, no. 5, pp. 3457–3469, May 2019.
[53] J. Yu, B. Cheng, C. Hang, Y. Hu, S. Liu, Y. Wang, and J. Shen, "A deep learning based RSA strategy for elastic optical networks," in *Proc. 18th Int. Conf. Opt. Commun. Netw. (ICOCN)*, Aug. 2019, pp. 1–3.
[54] A. P. Bianzino, L. Chiaraviglio, and M. Mellia, "GRiDA: A green distributed algorithm for backbone networks," in *Proc. IEEE Online Conf. Green Commun.*, Sep. 2011, pp. 113–119.
[55] E. Gelenbe and S. Silvestri, "Reducing power consumption in wired networks," in *Proc. 24th Int. Symp. Comput. Inf. Sci.*, Sep. 2009, pp. 292–297.
[56] L. Chiaraviglio, M. Mellia, and F. Neri, "Energy-aware networks: Reducing power consumption by switching off network elements," in *Proc. IEEE Int. Conf. Commun. Workshops*, May 2009, pp. 1–5.
[57] A. P. Bianzino, L. Chiaraviglio, and M. Mellia, "Distributed algorithms for green IP networks," in *Proc. IEEE INFOCOM Workshops*, Mar. 2012, pp. 121–126.
[58] A. Fallahpour, H. Beyranvand, S. A. Nezamalhosseini, and J. A. Salehi, "Energy efficient routing and spectrum assignment with regenerator placement in elastic optical networks," *J. Lightw. Technol.*, vol. 32, no. 10, pp. 2019–2027, May 15, 2014.
[59] P. Johannisson and E. Agrell, "Modeling of nonlinear signal distortion in fiber-optical networks," *J. Lightw. Technol.*, vol. 32, no. 23, pp. 4544–4552, Oct. 1, 2014.
[60] L. Yan, Y. Xu, M. Brandt-Pearce, N. Dharmaweera, and E. Agrell, "Regenerator site predeployment in nonlinear dynamic flexible-grid networks," in *Proc. Eur. Conf. Opt. Commun. (ECOC)*, no. 2, Sep. 2017, pp. 511–513.
[61] J. Mata, I. de Miguel, R. J. Durán, N. Merayo, S. K. Singh, A. Jukan, and M. Chamania, "Artificial intelligence (AI) methods in optical networks: A comprehensive survey," *Opt. Switching Netw.*, vol. 28, pp. 43–57, Apr. 2018.
[62] E. Q. Martins and M. M. Pascoal, "A new implementation of yen's ranking loopless paths algorithm," *Quart. J. Belg., Fr. Italian Oper. Res. Societies*, vol. 1, pp. 121–133, Jun. 2003.
[63] K. Christodoulopoulos, I. Tomkos, and E. Varvarigos, "Time-varying spectrum allocation policies and blocking analysis in flexible optical networks," *IEEE J. Sel. Areas Commun.*, vol. 31, no. 1, pp. 13–25, Jan. 2013.
[64] K. Christodoulopoulos, K. Manousakis, E. Varvarigos, and M. Angelou, "Considering physical layer impairments in offline RWA," *IEEE Netw.*, vol. 23, no. 3, pp. 26–33, May 2009.
[65] L. Yan, E. Agrell, M. N. Dharmaweera, and H. Wymeersch, "Joint assignment of power, routing, and spectrum in static flexible-grid networks," *J. Lightw. Technol.*, vol. 35, no. 10, pp. 1766–1774, May 15, 2017.
[66] D. Hillerkuss *et al.*, "Single-laser 32.5 Tbit/s Nyquist WDM transmission," *IEEE/OSA J. Opt. Commun. Netw.*, vol. 4, no. 10, pp. 715–723, Oct. 2012.
[67] Y. Zhou, Q. Sun, and S. Lin, "Link state aware dynamic routing and spectrum allocation strategy in elastic optical networks," *IEEE Access*, vol. 8, pp. 45071–45083, 2020.
[68] A. Rosa, C. Cavdar, S. Carvalho, J. Costa, and L. Wosinska, "Spectrum allocation policy modeling for elastic optical networks," in *Proc. High Capacity Opt. Netw. Emerg./Enabling Technol.*, Dec. 2012, pp. 242–246.
[69] B. C. Chatterjee, N. Sarma, and P. P. Sahu, "Priority based routing and wavelength assignment with traffic grooming for optical networks," *J. Opt. Commun. Netw.*, vol. 4, no. 6, p. 480, 2012.
[70] F. Lezama, G. Castañón, M. Sarmiento, and E. de Cote, "Solving routing and spectrum allocation problems in flexgrid optical networks using precomputing strategies," *Photonic Netw. Commun.*, vol. 40, no. 3, pp. 31–36, 2020.

KUSALA MUNASINGHE received the Bachelor of Engineering degree (Hons.) in electronics and telecommunication engineering, in 2017. She is currently pursuing the Master of Philosophy degree with the University of Sri Jayewardenepura, Sri Lanka. From 2018 to 2020, she worked as a Graduate Research Assistant with the National Research Council of Sri Lanka. She is also working as a Probationary Lecturer with the Department of Electronics and Telecommunication Engineering, Sri Lanka Technological Campus. Her research interests include optical communications, network optimization, and machine learning.

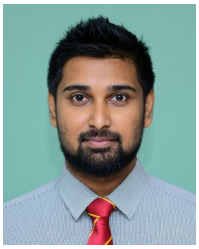

M. NISHAN DHARMAWEERA (Member, IEEE) received the Bachelor of Engineering degree (Hons.) in electrical and computer systems engineering, in 2009, and the Ph.D. degree in optical networks from Monash University, Malaysia, in 2014. From 2015 to 2016, he worked as a Postdoctoral Researcher with the FORCE Research Center, Chalmers University of Technology, Sweden. He joined the Department of Electrical and Electronic Engineering, University of Sri Jayewardenepura, as a Senior Lecturer. His research interests include optical communications, network optimization, applications of electromagnetics, and the Internet of Things.

UDITHA WIJEWARDHANA (Member, IEEE) received the Ph.D. degree in telecommunications engineering from the Centre for Wireless Communications, University of Oulu, Finland, in 2020. He is currently a Senior Lecturer with the Department of Electrical and Electronic Engineering, University of Sri Jayewardenepura. His research interests include application of optimization techniques for signal processing and wireless communications, compressed sensing, and machine learning.

CHAMITHA DE ALWIS (Member, IEEE) received the Ph.D. degree in electronic engineering from the University of Surrey, U.K., in 2014. He is currently a Senior Lecturer in electronic and telecommunication engineering with the University of Sri Jayewardenepura, Sri Lanka. His research interests include next generation networks, the IoT, and network security.

RAJENDRAN PARTHIBAN (Senior Member, IEEE) received the Bachelor of Engineering degree (Hons.), in 1997, and the Ph.D. degree in optical networks from the University of Melbourne, Australia, in 2004. He joined the School of Engineering, Monash University, Malaysia, as a Lecturer, in 2006. He is currently a Professor with the School of Engineering, where he has been working as the Deputy Head of School (Academic), since August 2010. He has over 80 journal and conference publications. He received external grants worth over RM 2 million. Twelve Ph.D. and one Master students have completed their studies under his supervision. His research interests include optical networks, visible light communications, vehicular communication, grid/cloud/fog computing, and engineering education. He is a Senior Member of the Optical Society (OSA).